A Journey from *n*-Heptane to Liquid Transportation Fuels. 1. The Role of the Allylic Radical and Its Related Species in Aromatic Precursor Chemistry

Hongzhi R. Zhang,* Eric G. Eddings, and Adel F. Sarofim

Department of Chemical Engineering, University of Utah, Salt Lake City, Utah 84112

Received August 31, 2007. Revised Manuscript Received November 16, 2007

The Utah normal heptane mechanism compiled from submechanisms in the literature was extended into a detailed normal decane combustion mechanism, which is a subset of the Utah surrogate mechanisms. Few species have greater impact on the concentrations of other species than the allyl radical $CH_2CH{=}CH_2$. Reactions involving the allyl radical and its isomers determine the concentration levels of all olefins, most higher unsaturated species, and benzene. To correctly predict the concentration of benzene, the reaction rates involving allyl-radical-related species need to be accurate and the concentration profiles of these species need to be satisfactory. Kinetic rates found in the literature are compared in the current work for various reference reactions that involve the allylic radicals. The improvements in numerical predictions of unsaturated species are achieved after a rigorous study in finding reliable reaction rates and kinetic correlations between various species. Some of these rates are adopted as the generic rates that have been used in the Utah surrogate mechanisms in previous studies. The modified mechanism is able to predict the concentration profiles of unsaturated species in *n*-decane and *n*-heptane flames with good numerical accuracy. The concentrations of these species are closely related to those of various allylic radicals, and reliable kinetics of allylic reactions are critical in predicting the concentrations of benzene and higher aromatics.

Introduction

Combustion chemistry of paraffinic components in real fuels has been developed by various researchers for compounds from *n*-heptane to *n*-hexadecane,[1–19] and was reviewed by Ranzi[20] and Simmie[21] and co-workers. Major efforts have been made in kinetic studies of real fuel combustion in order to map out the principal fuel decomposition pathways, because a complete gas phase model to be used in soot and aromatic species modeling should provide means for linking the decomposition of practical fuels with core reaction kinetics of the formation and consumption of C_2-C_4 aromatic precursors. An understanding of the chemistry of these precursor species, for example, the widely accepted benzene precursors (acetylene, propargyl and allyl radicals, allene and propyne, C_4H_5 and C_4H_3 isomers), is critical to predict the concentration of benzene correctly.

Some radicals play essential roles in bridging the decomposition chemistry of fuel molecules and the formation mechanism of first aromatic rings. For example, in the early studies of C_1-C_2 gas phase chemistry by Frenklach[22] and Westbrook[23] and co-workers, the vinyl radical $CH_2{=}CH\bullet$ was proposed to be the most important species for the emergence of carbon oxide combustion products (CO and CO_2). Vinyl radical was also suggested to be the intermediate to form another critical species—the propargyl radical $CH_2{=}C{=}CH\bullet \leftrightarrow \bullet CH_2{-}C{\equiv}CH$, the formation and consumption mechanism of which plays an important role in the formation of the first aromatic ring—phenyl radical C_6H_5 or benzene C_6H_6. The vinyl and propargyl radicals, therefore, form the two most active reaction centers that

* Corresponding author. E-mail: westshanghai@yahoo.com.

(1) Cathonnet, M.; Dagaut, P.; Chakir, A.; Boettner, J. C. *Trends Phys. Chem.* **1990**, *1* (1), 167.
(2) Bales-Gueret, C.; Cathonnet, M.; Boettner, J. C.; Gaillard, F. *Energy Fuels* **1992**, *6* (2), 189.
(3) Dagaut, P.; Reuillon, M.; Boettner, J.-C.; Cathonnet, M. *Proc. Combust. Inst.* **1994**, *25*, 919.
(4) Lindstedt, R. P.; Maurice, L. Q. *Combust. Sci. Technol.* **1995**, *107* (4–6), 317–353.
(5) Bollig, M.; Pitsch, H.; Hewson, J. C.; Seshadri, K. *Proc. Combust. Inst.* **1996**, *26*, 729.
(6) Pitsch, H.; Peters, N.; Seshadri, K. *Proc. Combust. Inst.* **1996**, *26*, 763.
(7) Doute, C.; Delfau, J.-L.; Vovelle, C. *Combust. Sci. Technol.* **1997**, *130* (1–6), 269.
(8) Held, T. J.; Marchese, A. J.; Dryer, F. L. *Combust. Sci. Technol.* **1997**, *123*, 107.
(9) Ranzi, E.; Faravelli, T.; Gaffuri, P.; Sogaro, A.; Danna, A.; Ciajolo, A. *Combust. Flame* **1997**, *108*, 24.
(10) Curran, H. J.; Gaffuri, P.; Pitz, W. J.; Westbrook, C. K. *Combust. Flame* **1998**, *114*, 149.
(11) Glaude, P. A.; Warth, V.; Fournet, R.; Battin-Leclerc, F.; Scacchi, G.; Come, G. M. *Int. J. Chem. Kinet.* **1998**, *30* (12), 949.
(12) Doute, C.; Delfau, J. L.; Vovelle, C. *Combust. Sci. Technol.* **1999**, *147*, 61.
(13) Battin-Leclerc, F.; Fournet, R.; Glaude, P. A.; Judenherc, B.; Warth, V.; Come, G. M.; Scacchi, G. *Proc. Combust. Inst.* **2000**, *28*, 1597.
(14) Bikas, G.; Peters, N. *Combust. Flame* **2001**, *126* (1–2), 1456.
(15) Fournet, R.; Battin-Leclerc, F.; Glaude, P. A.; Judenherc, B.; Warth, V.; Come, G. M.; Scacchi, G.; Ristori, A.; Pengloan, G.; Dagaut, P.; Cathonnet, M. *Int. J. Chem. Kinet.* **2001**, *33* (10), 574.
(16) Law, M. E.; Westmoreland, P. R.; Cool, T. A.; Wang, J.; Hansen, N.; Kasper, T. *Proc. Combust. Inst.* **2007**, *31*, 565.
(17) Zhang, H. R.; Eddings, E. G.; Sarofim, A. F. *Combust. Sci. Technol.* **2007**, *179* (1–2), 61–89.
(18) Zhang, H. R.; Eddings, E. G.; Sarofim, A. F. *Proc. Combust. Inst.* **2007**, *31*, 401–409.
(19) Zhang, H. R.; Huynh, L. K.; Kungwan, N.; Yang, Z.; Zhang, S. *J. Phys. Chem. A* **2007**, *111*, 4102–4115.
(20) Ranzi, E.; Dente, M.; Goldaniga, A.; Bozzano, G.; Faravelli, T. *Prog. Energy Combust. Sci.* **2001**, *27* (1), 99.
(21) Simmie, J. M. *Prog. Energy Combust. Sci.* **2003**, *29* (6), 599.
(22) Frenklach, M.; Warnatz, J. *Combust. Sci. Technol.* **1987**, *51*, 265.
(23) Marinov, N. M.; Pitz, W. J.; Westbrook, C. K.; Castaldi, M. J.; Senkan, S. M. *Combust. Sci. Technol.* **1996**, *211*, 116–117.

10.1021/ef700526n CCC: $40.75
Published on Web 01/04/2008

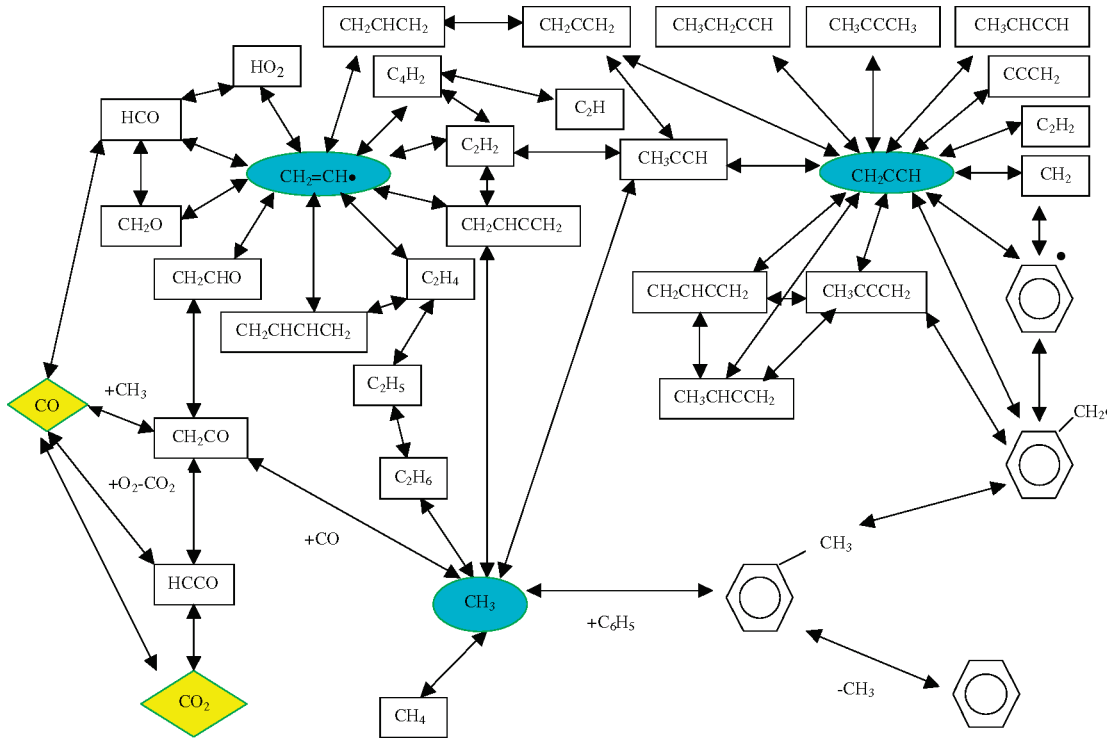

Figure 1. Critical reaction pathways for the gas phase chemistry of vinyl and propargyl radicals compiled from Frenklach and Westbrook reaction models. Rhombus boxes indicate the combustion product species, and oval boxes contain the active radical reaction centers.

Scheme 1

1. vinylic route:	fuel → primary alkyl radical → ethylene → vinyl radical
2. allylic route:	fuel → alkyl radical → olefin → allylic radical

coordinate fuel consumption, product formation, and other radical chemistry in the Frenklach and Westbrook gas phase chemical models, the major reactions of which are summarized in Figure 1. The vinylic aromatic precursor formation routes from C_2 (vinyl radical and acetylene) to C_3 (propargyl and allyl radicals, allene, and propyne) species in these two studies derived for small molecular fuels, however, are not adequate to describe the combustion chemistry of larger compounds such as those found in transportation fuels.

In addition to the vinylic route, a new decomposition route for real fuels from saturated (e.g., paraffins) to unsaturated (e.g., olefins) species to allylic radicals (designated as the allylic route in this work) is also important to benzene formation. It is noteworthy that the vinylic and allylic routes both contribute to the formation of critical aromatic precursors in practical fuel combustion systems (Scheme 1), because β scission reactions of primary alkyl radicals, the most abundant alkyl radicals from fuel decomposition, produce ethylene.[24]

The vinylic and allylic radicals and their products of C_2-C_4 species are the most important benzene precursors via two classes of reactions (Scheme 2): (1) combination reactions of $C_4 + C_2$[22,25] and (2) combination reactions of $C_3 + C_3$.[26]

The importance of the allylic route has been studied in an earlier study[18] on premixed flames burning real fuels of synthetic natural gas, gasoline, and kerosene. Our previous studies of combustion chemistry of large paraffinic fuels[17–19] were based upon the analysis of major reaction pathways of *n*-heptane.[24,27]

Scheme 2

Class 1,	R1:	$C_2H_2 + CH_2CHCHCH$	=	$C_6H_6 + H$
	R2:	$C_2H_2 + HCCHCCH$	=	C_6H_5
Class 2,	R3:	$H_2CCCH + H_2CCCH$	=	C_6H_6
	R4:	$H_2CCCH + CH_2CCH_2$	=	$C_6H_6 + H$
	R5:	$H_2CCCH + H_2CCCH$	=	$C_6H_5 + H$
	R6:	$H_2CCCH + CH_2CHCH_2$	=	FULVENE + 2H

A detailed discussion of the mechanism generation methodology was provided for reaction classes of paraffins (thermal decomposition and hydrogen abstraction), alkyl radicals (isomerization, β scission, and hydrogen abstraction by O_2), and olefins (hydrogen addition followed by β scission). Generic rates were assigned to reactions involving paraffins, olefins, and alkyl radicals in the same reaction classes with adjustments of the statistical factor and activation energy.

Rates of reactions involving alkynes, allylic radicals, and other unsaturated species were carefully estimated by consulting findings in the literature for the same or similar reactions. Inevitably, there are relatively higher uncertainties for reactions that involve allylic radicals in comparison with those using generic rates, although allylic radicals determine the concentrations of many important aromatic precursors such as propyne, butyne, butylene isomers, and most unsaturated compounds that contribute to the major formation routes of benzene. For example, numerical deviations were found in modeling results using the Utah heptane mechanism[24,27] for C_3-C_7 olefins by 30–50%, for benzene concentrations by a factor of 3, and for acetylenes by 30–80%.[28] The kinetic uncertainties and the

(24) Zhang, H. R.; Eddings, E. G.; Sarofim, A. F. *Energy Fuels* **2007**, *21* (2), 677–685.
(25) Westmoreland, P. R.; Dean, A. M.; Howard, J. B.; Longwell, J. P. *J. Phys. Chem.* **1989**, *93*, 8171.
(26) Miller, J. A.; Melius, C. F. *Combust. Flame* **1992**, *91*, 21.
(27) Zhang, H. R.; Eddings, E. G.; Sarofim, A. F.; Westbrook, C. K. Mechanism Reduction and Generation Using Analysis of Major Fuel Consumption Pathways for n-Heptane in Premixed and Diffusion Flames. *Energy Fuels* **2007**, *21* (4), 1967–1976.

importance of reactions that involve the allylic radical, however, have not been fully addressed in most published mechanisms developed for benzene prediction. Therefore, a detailed study is needed to provide resolutions of those areas of uncertainties.

In this paper, we will provide additional details on the improvement of the Utah heptane[24,27] mechanism that is included in the Utah surrogate mechanisms[17–19] in terms of the kinetic considerations of benzene precursors that inevitably involve allylic radicals and related species. The primary concerns of these species include the thermal decomposition of olefins, formation of minor olefinic species via combination involving allylic radicals, and evolution of other highly unsaturated species, which are important for the formation of benzene.

Experimental Data and Reaction Models

Simulation results using the Utah surrogate mechanisms have been compared favorably in earlier studies with experimental data of premixed flames of *n*-heptane (P = 760 Torr, Φ = 1.0 and 1.9),[17,24,27] isooctane (P = 760 Torr, Φ = 1.9), *n*-decane (P = 760 Torr, Φ = 1.7),[17] cyclohexane (P = 30 Torr, Φ = 1.0),[19] synthetic natural gas (P = 40 Torr, Φ = 1.0), gasoline (P = 760 Torr, Φ = 1.0), and kerosene (P = 760 Torr, Φ = 1.7),[18] and a jet stirred reactor with *n*-hexadecane (P = 760 Torr, Φ = 1.5),[17] and an opposed diffusion flame of *n*-heptane with a strain rate of 150 s^{-1} (fuel side 15% *n*-heptane and 85% N_2 at 338 K, 34.2 cm/s; air side at 298 K, 37.5 cm/s).[29] In the current study, the *n*-heptane (Φ = 1.9)[30] and *n*-decane (Φ = 1.7)[31] flames will be revisited to elaborate upon the importance of allylic reactions. The experimental uncertainties of species concentrations were estimated to be 10–20% for unsaturated species.[30] For the validation of the mechanism for these two flames, readers are directed to the above-mentioned references. Also, the mechanism discussed in this paper has been provided in the Supporting Information of ref 18. The importance of the reference reactions that will be discussed in the following sections very often depends on the fuel structural functionality, that is, the carbon number in this case (*n*-heptane versus *n*-decane), and the modifications of the continuously improved *n*-heptane mechanism in terms of numerical performance will be discussed. These reference reactions are listed in Table 1, together with kinetic rates taken from the combustion literature.

The simulator used for this study was CHEMKIN III,[32] and the thermodynamics data of species were obtained from the CHEMKIN thermodynamic database[33] or estimated by THERGAS[34] employing Benson's additivity theory. The transport properties of species were

Table 1. Rates of Reference Reactions Found in the Literature (Units of mole-cm-s-K-cal)

			rate coefficient		
A	n	E	1000 K	1500 K	ref
1. Olefin = Allyl + Alkyl Radicals					
7.94×10^{15}	0	70800	2.67	3.84×10^{5}	*a*
1.00×10^{16}	0	71300	2.61	4.08×10^{5}	*b*
1.00×10^{16}	0	71000	3.03	4.51×10^{5}	*c*
1.00×10^{19}	*−1*	*73400**	0.91	1.34×10^{5}	*d*
3.16×10^{16}	0	80927*	0.065	5.10×10^{4}	*e*
1.00×10^{16}	0	80000	0.033	2.20×10^{4}	*f*
5.00×10^{9}	0	44216	1.08	1.80×10^{3}	*g*
1.80×10^{15}	0	75050	0.071	2.09×10^{4}	*h*
2. 1-Butylene = Allyl + Methyl					
1.00×10^{16}	0	73000	1.11	2.31×10^{5}	*i*
2.50×10^{13}	0	63000	0.43	1.66×10^{4}	*j*
5.00×10^{15}	0	71000	1.52	2.26×10^{5}	*c*
2.50×10^{16}	0	77000	0.37	1.51×10^{5}	*k*
1.00×10^{19}	−1	73400	0.91	1.34×10^{5}	*d*
3.16×10^{16}	0	80869*	0.067	5.20×10^{4}	*e*
8.00×10^{16}	0	73375	7.34	1.63×10^{6}	*l*
2.50×10^{16}	0	75500	0.79	2.49×10^{5}	*m*
3. Allyl + Methyl = 1-Butylene					
1.00×10^{14}	−0.32	−131	1.17×10^{13}	1.01×10^{13}	*n*
5.00×10^{12}	0	0*	5.00×10^{12}	5.00×10^{12}	*c*
1.76×10^{50}	*−11*	*18600**	1.51×10^{13}	3.97×10^{12}	*d*
4. 2-Butylene = 1-Propenyl + Methyl					
1.00×10^{16}	0	80000	0.033	2.20×10^{4}	*f*
3.16×10^{17}	0	99288	6.29×10^{-5}	1.08×10^{3}	*i*
2.00×10^{16}	0	95000	3.44×10^{-5}	2.87×10^{2}	*o*
5.00×10^{16}	0	91000*	6.45×10^{-4}	2.75×10^{3}	*p*
5. Isobutylene = 2-Propenyl + Methyl					
1.92×10^{66}	−14.22	128100	4.21×10^{-5}	2.84×10^{2}	*q*
5.00×10^{16}	0	101000	4.20×10^{-6}	9.60×10^{1}	*k*
5.00×10^{18}	−1	73445	0.443	6.62×10^{4}	*r*
5.00×10^{16}	0	91500*	5.01×10^{-4}	2.32×10^{3}	*p*
6. Vinyl = Acetylene + H					
3.87×10^{8}	1.63	37058	2.39×10^{5}	2.32×10^{8}	*s*
2.00×10^{14}	0	39740*	4.12×10^{5}	3.24×10^{8}	*t*
6.93×10^{12}	0	44411	1.36×10^{3}	2.36×10^{6}	*u*
1.00×10^{13}	0	41105	1.04×10^{4}	1.02×10^{7}	*v*
3.16×10^{12}	0	38295	1.35×10^{4}	8.31×10^{6}	*i*
1.60×10^{14}	0	38000	7.92×10^{5}	4.65×10^{8}	*w*
2.03×10^{15}	−0.42	44460	2.14×10^{4}	3.12×10^{7}	*c*
7. 1-Propenyl = Propyne + H					
3.98×10^{12}	0	36495*	4.20×10^{4}	1.91×10^{7}	*i*
1.08×10^{15}	−0.6	38490	6.59×10^{4}	3.29×10^{7}	*c*
6.93×10^{12}	0	44383	1.38×10^{3}	2.36×10^{6}	*x*
3.98×10^{12}	0	36472	4.25×10^{4}	1.93×10^{7}	*d*
8. C_6H_{12}-1 + H = C_6H_{11} + H_2					
3.70×10^{13}	0	3900*	5.20×10^{12}	1.00×10^{13}	*c*
2.06×10^{14}	0	7925	3.82×10^{12}	1.44×10^{13}	*k*
9.14×10^{6}	2	5000	7.38×10^{11}	3.84×10^{12}	*y*
1.00×10^{14}	0	3500	1.72×10^{13}	3.09×10^{13}	*m*
1.30×10^{6}	2.4	4470	2.17×10^{12}	1.22×10^{13}	*z*
8.02×10^{13}	*0*	*3400**	1.45×10^{13}	2.56×10^{13}	*d*

* Rates in italic form are used in the Utah heptane mechanism before modification of allylic reactions; rates underlined are used in this work for the Utah surrogate mechanisms. [a] The reference species are 1-hexene[47,48] and 1-pentene.[49] [b] The reference species is 1-pentene.[50] [c] Curran et al.[10] [d] El Bakali et al.[30] [e] Doute et al., 1997;[7] this work; generic rate in Zhang et al., 2007.[17] [f] The reference species is 2-butylene.[51] [g] The reference species is 4-methyl 1-pentene.[52] [h] The reference species is 1-hexene.[36] [i] Dean, 1985.[39] [j] Sehon and Szwarc, 1950.[53] [k] Ranzi et al., 1997.[9] [l] Bikas and Peters, 2001;[14] Bollig et al., 1996.[5] [m] Allara and Shaw, 1980.[54] [n] Tsang, 1991.[37] [o] Konnov, 2000.[42] [p] This work. [q] Wang et al., 1999.[38] [r] Richter et al., 2005.[55] [s] Knyazev and Slagle, 1996;[56] Ranzi et al., 1997.[9] [t] Baulch et al., 1992;[40] Bollig et al., 1996;[5] Bikas and Peters, 2001.[14] [u] Rao and Skinner, 1988;[57] Doute et al., 1997.[7] [v] Manion and Louw, 1988.[58] [w] Warnatz, 1984.[59] [x] Doute et al., 1997.[7] [y] Bikas and Peters, 2001.[14] [z] Held et al., 1997.[8]

(28) Zhang, H. Numerical Combustion of Commercial Fuels and Soot Formation. Ph.D. dissertation, Department of Chemical Engineering, University of Utah, 2005.

(29) Zhang, H. R.; Yang, Z.; Eddings, E. G.; Sarofim, A. F. *Prepr. Symp.—Am. Chem. Soc., Div. Fuel Chem.* **2007**, *52* (1), 144–147.

(30) El Bakali, A.; Delfau, J. L.; Vovelle, C. *Combust. Flame* **1999**, *118*, 381.

(31) Doute, C.; Delfau, J.-L.; Akrich, R.; Vovelle, C. *Combust. Sci. Technol.* **1995**, *106* (1–6), 327.

(32) Kee, R. J.; Rupley, F. M.; Miller, J. A.; Coltrin, M. E.; Grcar, J. F.; Meeks, E.; Moffat, H. K.; Lutz, A. E.; Dixon-Lewis, G.; Smooke, M. D.; Warnatz, J.; Evans, G. H.; Larson, R. S.; Mitchell, R. E.; Petzold, L. R.; Reynolds, W. C.; Caracotsios, M.; Stewart, W. E.; Glarborg, P.; Wang, C.; Adigun, O.; Houf, W. G.; Chou, C. P.; Miller, S. F. *Chemkin Collection*, release 3.7.1; Reaction Design, Inc: San Diego, CA, 2003.

(33) Kee, R. J.; Rupley, F. M.; Miller, J. A. The Chemkin thermodynamic database; Sandia Report #SAND 87-8215B, 1993.

(34) Muller, C.; Michel, V.; Scacchi, G.; Côme, G. M. *J. Chim. Phys.* **1995**, *92*, 1154.

(35) Kee, R. J.; Dixon-Lewis, G.; Warnatz, J.; Coltrin, M. E.; Miller, J. A. The Chemkin transport database; Sandia Report #SAND 86-8246, 1986.

(36) Yahyaoui, M.; Djebaili-Chaumeix, N.; Paillard, C.-E.; Touchard, S.; Fournet, R.; Glaude, P. A.; Battin-Leclerc, F. *Proc. Combust. Inst.* **2005**, *30*, 1137–1145.

(37) Tsang, W. *J. Phys. Chem. Ref. Data* **1991**, *20* (2), 221.

(38) Wang, S.; Miller, D. L.; Cernansky, N. P.; Curran, H. J.; Pitz, W. J.; Westbrook, C. K. *Combust. Flame* **1999**, *118* (3), 415.

obtained from the CHEMKIN transport database[35] or estimated from those of similar species.

Reaction of Allylic Radicals and Related Species

1. Olefin Thermal Decomposition Reactions. Thermal decomposition of paraffin species is usually not a preferred decomposition pathway except at very high temperatures.[27] Under premixed flame conditions, fuels are usually depleted when high temperatures are reached. The thermal decomposition of large olefins, however, is one of their major consumption routes[24] because of the higher flame temperatures at which olefin species reach their maximum concentrations, in addition to the stabilizing effects of allylic radicals with two resonant structures, which infers an increase in thermal decomposition rate constants. For example, olefin species reach their maximum concentrations at 1200 K in the reaction zone where fuels are completely depleted in the *n*-heptane and *n*-decane flames studied earlier.[17] Therefore, it is necessary to obtain reliable rates of olefin thermal decomposition reactions in combustion modeling.

There are two groups of rates available in the literature of olefin thermal decomposition, as shown in Table 1 for reaction 1. One group of data has a rate at 1500 K of the order of 10^5 s^{-1}, and the other group, of the order of 10^4 s^{-1}. The higher rates were proposed for temperatures near 1000 K, and the lower rates were obtained for higher temperatures of 1300–1400 K. Yahyaoui and co-workers[36] (A, n, $E = 1.8 \times 10^{15}$, 0, 75050, units specified in Table 1) pointed out from their 1-hexene shock tube experimental data that the olefin thermal decomposition rate has a smaller prefactor and a higher energy barrier at higher temperatures. The rate used in the Utah heptane mechanism is adopted from El Bakali et al.[30] (A, n, $E = 1 \times 10^{19}$, -1, 73400) in their *n*-heptane mechanism (this mechanism was adopted in the Utah *n*-heptane mechanism), which was reduced in their *n*-decane mechanism[7] for olefins of 1-octene and 1-heptene (A, n, $E = 3.16 \times 10^{16}$, 0, 80927). Although 81 kcal/mol is considerably higher than most values in the literature, the same modification was adopted in the Utah surrogate mechanism, because the predicted olefin concentrations using the Utah heptane mechanism are consistently lower than the measured values in the *n*-heptane and *n*-decane flames for almost every species as shown in Figures 2 and 3. It is noted that the new rate used in the modified mechanism has a higher prefactor also, and is very close to the latest Yahyaoui rate, as shown in Table 1. Although olefin formation kinetics might also be responsible for their underestimation, the concern is less important because different olefins are formed via different reaction classes.[24] For example, nonconjugate olefins are generated dominantly from β scission reactions of alkyl radicals with well-known rate information; and hydrogen abstraction with O_2 from conjugate alkyl radicals is the major route toward conjugate olefins. It is noted that concentrations of olefins are consistently underpredicted, independent of the formation routes. The consumption rates of olefins in these two flames, therefore, are probably too high.

Heptenes and 1-Hexene. The predicted maximum concentration of 1-heptene is lower than the measured value in the *n*-heptane flame by 33% of its MPC (measured peak concentration, a normalized concentration presentation). A modification of the thermal decomposition rate of 1-heptene for the formation of allyl and primary butyl radical (using the Doute rate) was found to be critical in narrowing the deviation, and the peak concentration increases by 19% of its MPC. The new rate is used as the generic rate for thermal decomposition reactions for other olefins also.[17] The predicted maximum concentration of 1-heptene is about 14% lower after the modification of the rates of allylic reactions. With a few minor modifications, the peak concentration of 1-heptene in the *n*-heptane flame is underpredicted by only 11%, as shown in Figure 2.

The generic rate for thermal decomposition was used for other olefin species in the *n*-heptane and *n*-decane flames, and a similar trend was observed for each species, as shown in Figure 2. The predicted maximum concentrations of 2-heptene and 3-heptene in the *n*-heptane flame are 20% lower and 33% higher than the measured values, respectively. The new thermal decomposition rates increase the predictions of 2- and 3-heptenes by 40 and 94% of the MPC, respectively. The excessive gain of 3-heptene concentrations was counterbalanced by new consumption reactions mainly of hydrogen addition followed by decomposition, the discussion of which is available elsewhere.[28] For example, 3-heptene can decompose to 1-pentene and ethyl radical by the addition of a hydrogen radical, C_7H_{14}-3 + H = C_5H_{10}-1 + C_2H_5. The final predicted concentrations of 2- and 3-heptenes are 19 and 27% higher than the measured values, respectively. The higher predictions reflect the less complete reaction sets of the two olefins with possibly missing consumption routes. In the *n*-decane flame, a similar modification yields a gain of 44% of the MPC for the peak concentration of 1-heptene, which narrows its numerical deviation from 44%

(39) Dean, A. M. *J. Phys. Chem.* **1985**, *89*, 4600.
(40) Baulch, D. L.; Cobos, C. J.; Cox, R. A.; Esser, C.; Frank, P.; Just, Th.; Kerr, J. A.; Pilling, M. J.; Troe, J.; Walker, R. W.; Warnatz, J. *J. Phys. Chem. Ref. Data* **1992**, *21*, 411.
(41) Curran, H. J.; Gaffuri, P.; Pitz, W. J.; Westbrook, C. K. *Combust. Flame* **2002**, *129* (3), 253.
(42) Konnov, A. A. *Eurasian Chem.-Technol. J.* **2000**, *2* (3–4), 257.
(43) Laskin, A.; Wang, H. *Chem. Phys. Lett.* **1999**, *303* (1–2), 43.
(44) Leung, K. M.; Lindstedt, R. P. *Combust. Flame* **1995**, *102* (1–2), 129.
(45) Davis, S. G.; Law, C. K.; Wang, H. *Combust. Flame* **1999**, *119* (4), 375.
(46) Marinov, N. M.; Pitz, W. J.; Westbrook, C. K.; Vincitore, A. M.; Castaldi, M. J.; Senkan, S. M.; Melius, C. F. *Combust. Flame* **1998**, *114* (1–2), 192.
(47) King, K. D. Very Low-Pressure Pyrolysis (VLPP) of Hex-1-ene. Kinetics of the Retro-ene Decomposition of a Mono-Olefin. *Int. J. Chem. Kinet.* **1979**, *11*, 1071.
(48) Tsang, W. Thermal Stability of Cyclohexane and 1-Hexene. *Int. J. Chem. Kinet.* **1978**, *10*, 1119.
(49) Brown, T. C.; King, K. D.; Nguyen, T. T. Kinetics of primary processes in the pyrolysis of cyclopentanes and cyclohexanes. *J. Phys. Chem.* **1986**, *90*, 419.
(50) Tsang, W. Thermal Decomposition of Cyclopentane and Related Compounds. *Int. J. Chem. Kinet.* **1978**, *10*, 599.
(51) Jeffers, P.; Bauer, S. H. The Homogeneous Pyrolysis of 2-Butenes. *Int. J. Chem. Kinet.* **1974**, *6*, 763.
(52) Taniewski, M. Kinetics and mechanism of the thermal decomposition of 4-methylpent-1-ene. *J. Chem. Soc.* **1965**, 7436–7443.
(53) Sehon, A. H.; Szwarc, M. The CH2:CH2-CH3 bond dissociation energy and the heat of formation of the allyl radical. *Proc. R. Soc. London, Ser. A* **1950**, *202*, 263–276.
(54) Allara, D. L.; Shaw, R. A compilation of kinetic parameters for the thermal degradation of n-alkane molecules. *J. Phys. Chem. Ref. Data* **1980**, *9* (3), 523.
(55) Richter, H.; Granata, S.; Green, W. H.; Howard, J. B. Detailed modeling of PAH and soot formation in a laminar premixed benzene/oxygen/argon low-pressure flame. *Proc. Combust. Inst.* **2005**, *30* (Pt. 1), 1397–1405.
(56) Knyazev, V. D.; Slagle, I. R. Experimental and theoretical study of the C2H3 = H + C2H2 reaction. Tunneling and the shape of falloff curves. *J. Phys. Chem.* **1996**, *100*, 16899–16911.
(57) Rao, V. S.; Skinner, G. B. Reactions of vinyl radicals at high temperatures: Pyrolysis of vinyl bromide and vinyl iodide and the reaction H + C2D2 = D + C2HD. *J. Phys. Chem.* **1988**, *92*, 6313.
(58) Manion, J. A.; Louw, R. Gas-phase hydrogenolysis of chloroethene: Rates, products, and computer modeling. *J. Chem. Soc., Perkin Trans. 2* **1988**, *8*, 1547–1555.
(59) Warnatz, J. Rate coefficients in the C/H/O system. In *Combustion Chemistry*; Gardiner, W. C., Jr., Ed.;Springer-Verlag: New York, 1984.

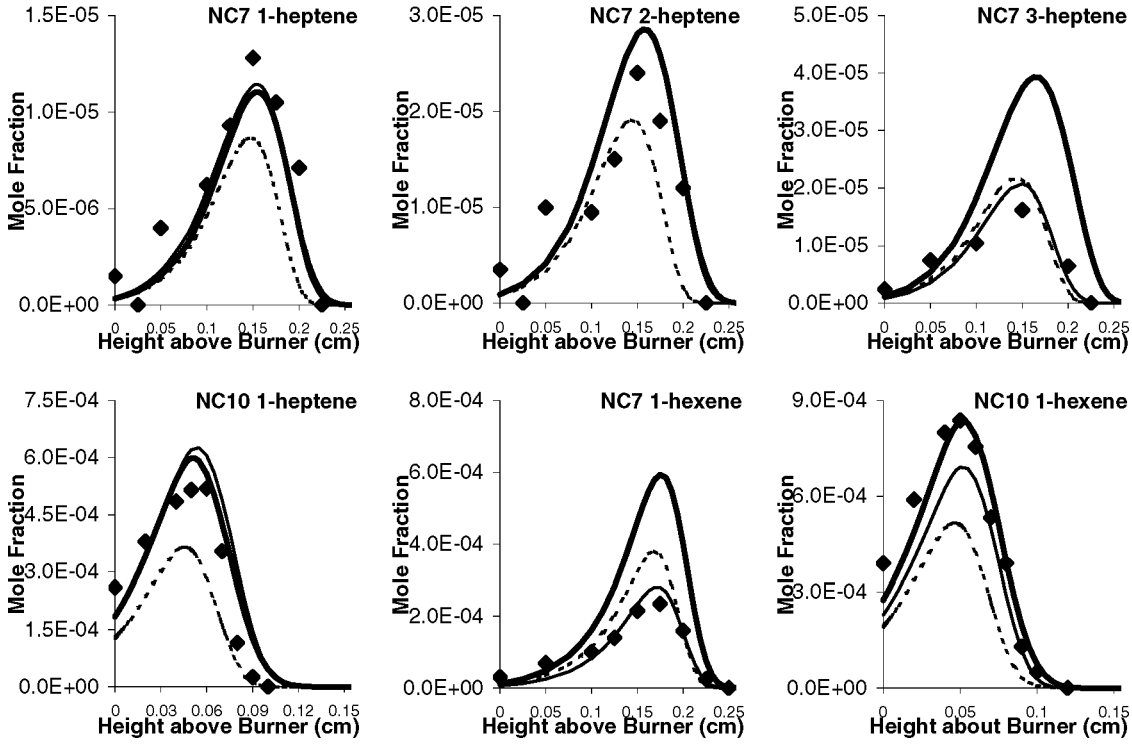

Figure 2. Numerical effects of modifications of allylic reactions on the concentration profiles of heptene isomers and 1-hexene in the *n*-heptane and the *n*-decane flames depicted by the differences between the predicted results before (dotted lines) and after (heavy solid lines) the modifications of the allylic reactions. The symbols represent the experimental data; the predicted results using the final Utah surrogate mechanisms are represented by the thin solid line. In the case of NC7 2-heptene, the thin and heavy lines overlap completely.

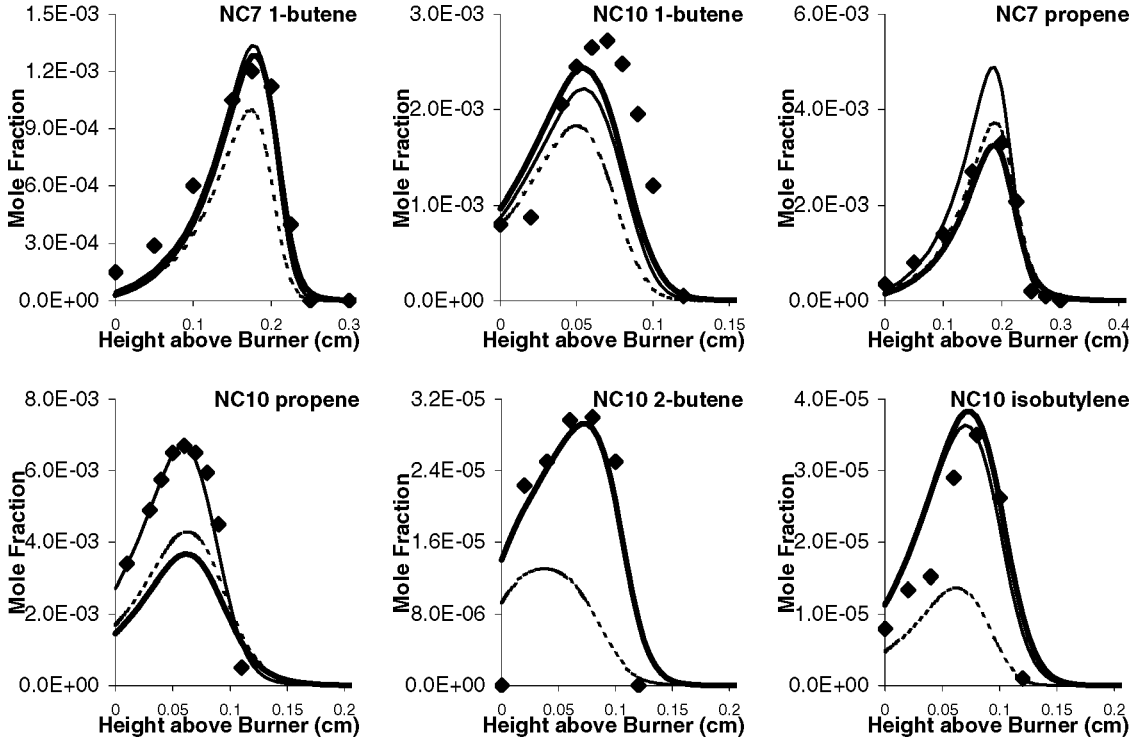

Figure 3. Numerical effects of modifications on the concentration profiles of 1-butylene in the *n*-heptane and the *n*-decane flames illustrated by the differences between the predicted results before (dotted lines) and after (heavy solid lines) the modifications of the allylic reactions. The symbols represent the experimental data; the predicted results using the final Utah surrogate mechanisms are represented by the thin solid line. In the case of NC10 2-butylene, the thin and heavy solid lines overlap completely.

underprediction to 21% overprediction. The predicted profile of 1-hexene is improved also as the overprediction of the maximum is reduced from 62 to 19% in the *n*-heptane flame, and the underprediction of the peak concentration is narrowed from 48 to 18% in the *n*-decane flame. As shown in Figure 2, the modified thermal decomposition rate is the main reason for the improved prediction, especially in the *n*-decane flame. A few new reactions mainly of hydrogen addition followed by

decomposition, similar to the treatment for 3-heptene, are needed, in addition to the modified thermal decomposition rate, to yield a closer prediction.

1-Butylene. The thermal decomposition of 1-butylene (reaction 2 in Table 1) was written in the Utah *n*-heptane mechanism as its reverse combination reaction (reaction 3 in Table 1) with the rate adopted from El Bakali et al.[30] As shown in Table 1, the combination rates found in the literature are very close to each other. The reverse rate calculated from thermodynamics, however, shows a significant deviation from the generic rate for this class, which indicates the complexity in the potential energy surface and other kinetic considerations that involve a methyl radical. Two irreversible 1-butylene reactions of decomposition (using the generic rate) and combination (using the rate by Tsang[37]), therefore, were included in the modified mechanism. The maximum concentrations of 1-butylene increase by 17 and 20% for the *n*-decane and *n*-heptane flames, respectively. The modification is the main contributor to reducing the underprediction of 1-butylene from 53% in the *n*-decane flame to 18% and to narrowing the deviation in the *n*-heptane flame from −17 to +12%, as shown in Figure 3.

Propylene. The Utah heptane mechanism underpredicts the peak propylene concentration by 44% in the *n*-decane flame and overpredicts it by 7% in the *n*-heptane flame. The modified reaction rate of 1-butylene thermal decomposition (reactions 2 and 3 in Table 1) in favor of 1-butylene formation at the cost of C_3 species indirectly lowers the predicted peak concentration of propylene in the *n*-decane and *n*-heptane flames by 4 and 5% of the MPC, respectively. Other added or modified reactions enable the extended mechanism to predict the peak concentration of propylene in the *n*-decane flame with a discrepancy of only +0.15%. However, those changes increase the concentrations of propylene significantly in the *n*-heptane flame with the maximum concentration overpredicted by 34%. The impact, although negative, of the modification of allylic reactions on the concentrations of propylene is illustrated in Figure 3.

2. Olefin Formation via Combination of Allyl-Related Radicals. In general, olefins with a terminal double bond are produced via β scission of alkyl radicals, and their carbon structure must be a possible fragment of the fuel molecule. New formation routes should be sought for olefins that cannot completely superimpose with any part of the fuel molecule, e.g., isobutylene in normal paraffin flames, or those with inner double bonds, e.g., 2-butylene.

2-Butylene. The predicted peak concentration of 2-butylene in the *n*-decane flame using the Utah heptane mechanism is 52% lower than the measured value. Predicting the concentrations of C_3H_5 isomers is important for 2-butylene, since the isomerization of 1-butylene via the 3-butenyl radical is one of the major formation routes of 2-butylene in the Utah heptane mechanism; furthermore, the level of 1-butylene is sensitive to changes in reactions involving C_3H_5 isomers. In general, the predicted 2-butylene concentrations increase with those of C_3H_5 species.

Major changes in isobutylene come from the reverse three new combination reactions of the C_3H_5 isomers and the methyl radical. The reactions involving 2-propenyl and 3-propenyl (allyl) radicals are assigned the rate of a similar decomposition reaction of isobutylene into the 2-propenyl and methyl radicals (reaction 5 in Table 1) used in the LLNL neo-pentane mechanism.[38] A faster rate is assigned to the decomposition reaction to form the 1-propenyl (CH_3—CH═CH•) and methyl radicals (reaction 4 in Table 1), since the 1-propenyl radical is the direct decomposition product of 2-butylene without any intramolecular hydrogen migrations. We first estimate rate constants of 2-butylene decomposition to form a 1-propenyl radical at different temperatures, which leads to a good fit of the experimental 2-butylene profile. Then, we decide the rate expression that best describes these temperature-dependent rate constants. The proposed rate expression is reported in Table 1. The rate is 1 order of magnitude higher than those of the reactions involving the other two C_3H_5 isomers and is close to those suggested by Dean[39] at higher temperatures. At 1200 K, the new rate is about 25% of the generic rate of the thermal decomposition of olefins (reaction 1 in Table 1) to account for the unstable chemical nature of 1-propenyl radical as compared to that of the allylic radical. The new reaction involving the 1-propenyl radical increases the predicted maximum concentration of 2-butylene in the *n*-decane flame by 45% of the MPC, and the other two new reactions involving 2- and 3-propenyl radicals provide an additional increase of 4% of the MPC. The extended mechanism yields a predicted peak concentration of 2-butylene in the *n*-decane flame only 2.67% lower than the measured value. The better predicted peak concentration of 2-butylene is mainly due to the modifications of allyl-related reactions, as shown in Figure 3.

Isobutylene. The predicted peak concentration of isobutylene in the *n*-decane flame using the Utah heptane mechanism is 80% lower than the measured value. Like the other butylene isomers, isobutylene is formed mainly from the combination of the propenyl isomers and methyl radical in the *n*-decane flame and its concentration will change with those of C_3 species. For example, the predicted peak concentration of isobutylene is reduced slightly by 3% of the MPC when the thermal decomposition rate of 1-butylene is modified (reactions 2 and 3 in Table 1), to include the conversion of allyl radical to 1-butylene.

Like the conversion reaction of 3-propenyl (allyl) radical to 1-butylene and that of 1-propenyl radical to 2-butylene, the other C_3H_5 isomer of the 2-propenyl radical directly forms isobutylene by combining with a methyl radical without intramolecular hydrogen migrations. The reaction is written in the irreversible decomposition form in the Utah heptane mechanism and gave satisfactory isobutylene prediction when the mechanism was tested with a premixed isooctane flame; and the reaction proceeds in the decomposition direction due to the abundance of isobutylene as the immediate product of the isooctane decomposition. The irreversible form, however, blocks the most important formation route of isobutylene via combination of the propenyl isomers and methyl radical when the fuel has no iso-C_4 substructures, for example, straight chain paraffins and other smaller fuels. The reversible decomposition reaction of isobutylene replaced the irreversible one using a rate similar to that used for 2-butylene (reaction 4 in Table 1) but with an adjustment in the activation energy. An extra 500 cal in the energy barrier is found to yield a better predicted peak concentration of isobutylene probably because isobutylene has the highest chemical stability among all three butylene isomers, since the electron-releasing effect of alkyl groups satisfies the electron-withdrawing properties of the sp^2-hybridized carbon atoms of the double bond. The new reversible decomposition reaction increases the predicted peak concentration of isobutylene in the *n*-decane flame by 65% of the MPC. Also, two new decomposition reactions of isobutylene to form the other two C_3H_5 isomers via intramolecular hydrogen migrations are added using the generic rate included in the LLNL neo-pentane mechanism,[38] and a minor increase of 5% of the MPC is seen for the level of isobutylene.

With those major modifications and a few minor ones, the predicted peak concentration of isobutylene in the *n*-decane

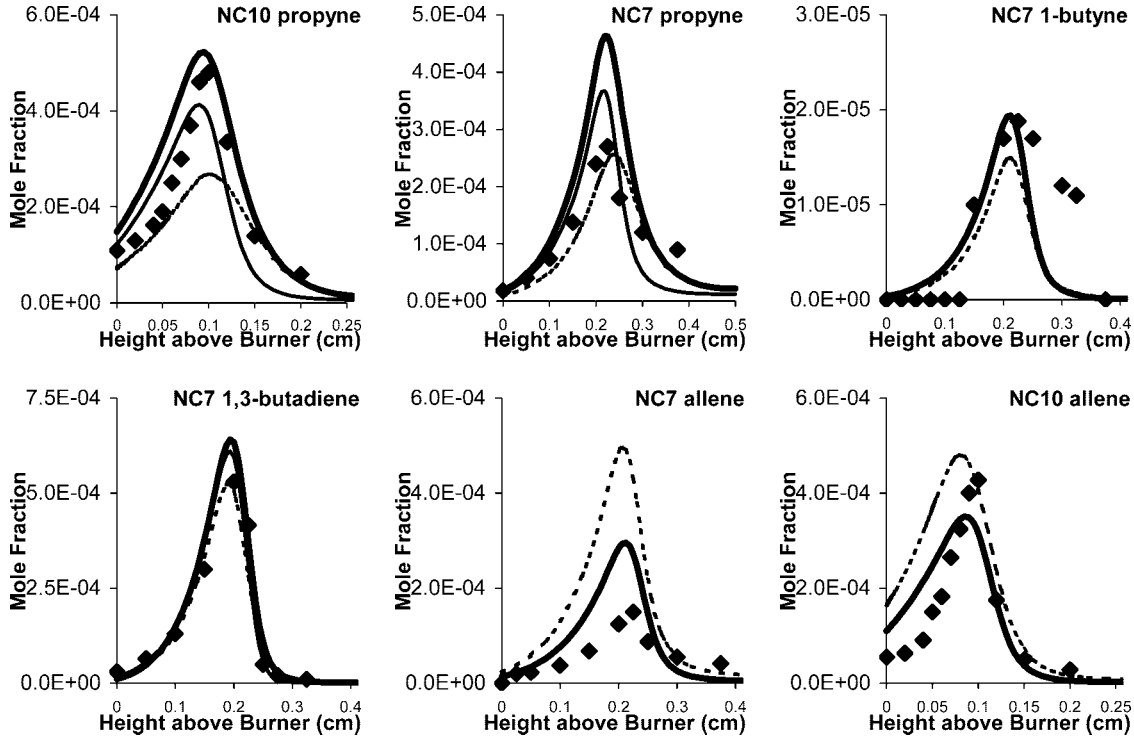

Figure 4. Numerical effects of modifications on the concentration profiles of higher unsaturated species in the *n*-heptane and the *n*-decane flames illustrated by the differences between the predicted results before (dotted lines) and after (heavy solid lines) the modifications of the allylic reactions. The symbols represent the experimental data; the predicted results using the final Utah surrogate mechanisms are represented by the thin solid line. The thin and heavy solid lines superimpose on each other for propyne, 1-butyne, and allene in both flames.

flame is only 4% higher than the experimental value, as seen in Figure 3. The better predicted peak concentration of isobutylene is mainly due to the modifications of allyl-related reactions.

3. Reactions of Highly Unsaturated Species with Allylic Radicals. The allylic radical has an electron deficiency that is between olefins (electron deficiency = 1) and alkynes and dienes (=2), enynes (=3), and diynes (=4). Therefore, allylic radicals are common intermediates for the formation of many highly unsaturated species in combustion systems that are major aromatic precursors.

Propyne. The predicted peak concentrations of propyne in the *n*-decane and the *n*-heptane flames using the Utah heptane mechanism are 81 and 52% lower than the measured values, respectively. The concentrations of propyne fluctuate with that of the allyl radical. For example, higher levels of terminal olefins due to the modification of reaction 1 in Table 1 increase the formation rate of propyne via the intermediate allyl radical formed from thermal decomposition of these larger olefins. On the other hand, the peak concentrations of propyne decrease by 4 and 6% of the MPC, respectively, in the *n*-decane and *n*-heptane flames after the change in the thermal decomposition reaction of 1-butylene, since the level of allyl radical is lowered to boost the concentrations of 1-butylene. Also, the decreased vinyl radical concentration due to the modification of the reaction rate of the unimolecular vinyl dehydrogenation (reaction 6 in Table 1) significantly reduces the level of propyne in the *n*-decane and *n*-heptane flames by 21 and 31% of the MPC, respectively, since the combination of the vinyl and methyl radicals is one of the most important formation routes of the allyl radical. The reaction written in the combination form of acetylene and hydrogen in the Utah heptane mechanism was replaced by its reverse reaction in the modified mechanism using the Baulch et al. rate,[40] which is only slightly higher than the Knyazev and Slagle rate[56] and slightly lower than the Warnatz rate.[59] The modification leads to significantly better predictions of acetylene concentrations in various flames, the discussion of which is presented elsewhere.[28]

Significant changes in the concentrations of propyne occur after reactions involving propyne are modified and new reactions are added. To provide a complete formation set of propyne from C_3H_5 isomers, a new dehydrogenation reaction of the 1-propenyl radical (CH_3—CH═CH•, reaction 7 in Table 1) is added using the rate proposed by Dean,[39] as most of the rates found in the literature are quite close to each other. The addition results in increases of the predicted peak concentrations of propyne of 26 and 38% of the MPC in the *n*-decane and *n*-heptane flames, respectively. Another dehydrogenation reaction of 2-propenyl radical (CH_3—C•═CH_2) was changed to a pseudo-first-order reaction so that it proceeds without the presence of a third body species. This approach of excluding third body species was employed in mechanisms of paraffins such as, among others, the LLNL normal heptane and isooctane[10,41] and the Vovelle decane[7] mechanisms and those proposed by Konnov,[42] Laskin,[43] Leung,[44] and Davis[45] and their co-workers; by contrast, this reaction retained the use of the third body species in other mechanisms such as the Milan[20] and the Marinov et al. butane[46] mechanisms. The reaction without the participation of a third body species yields increases in propyne concentrations of 27 and 38% of the MPC in the *n*-decane and *n*-heptane flames, respectively. With those changes and a few other ones, the predicted concentrations of propyne increase significantly using the extended mechanism, and its peak concentration is underpredicted by 14% in the *n*-decane flame and overpredicted by 36% in the *n*-heptane flame, as seen in Figure 4.

1-Butyne. The predicted maximum concentration of 1-butyne using the Utah heptane mechanism is 81% higher than the measured value in the *n*-heptane flame. The prediction of 1-butyne is also affected by changes made in allylic reactions. For example, the reductions in the level of allyl radicals by

modifying the olefin thermal decomposition rate (reaction 1 in Table 1) have negative impacts on the concentrations of 1-butyne because the change in the allyl radical concentration affects that of the propargyl radical, a species that contributes to the most important formation route of 1-butyne via a combination with the methyl radical. The higher concentrations of propyne after changes in reactions involving C_3H_5 isomers, for example, reaction 7 in Table 1, create more propargyl radicals via the hydrogen abstraction from propyne, and in turn increase the level of 1-butyne. Also, the predicted peak concentration of 1-butyne increases by 18% of the MPC because of the increased propargyl radical concentrations after the reductions in the formation rates of benzene via the combination of propargyl and allyl radicals. A detailed discussion of the benzene chemistry is beyond the scope of this work, and will be properly presented in a future publication. The changes in the concentrations of C_4 species such as 1-butylene and 1,3-butadiene also affect the level of 1-butyne formed via intermediate allylic C_4H_7 isomers. Although the modifications of allylic reactions do not contribute significantly to reducing the numerical deviation of 1-butyne, the extended mechanism overpredicts the peak concentration of 1-butyne in the *n*-heptane flame by only 3% with a few other modifications that were discussed elsewhere.[28]

1,3-Butadiene. The peak concentration of 1,3-butadiene using the Utah heptane mechanism in the *n*-heptane flame is underpredicted by 1%. No direct modifications were intended to improve the already good numerical results of 1,3-butadiene; however, the concentration of 1,3-butadiene is affected by changes in reactions involving other species. For example, the modifications in reactions of the lumped hexenyl radical, a higher allylic radical, will affect the concentration profile of 1,3-butadiene, since the decomposition of higher allylic radicals is one of the major formation routes of 1,3-butadiene. The rates found in the literature for 1-hexene reactions with a hydrogen radical are listed under reaction 8 in Table 1. The Curran et al.[10] rate is adopted in the modified mechanism, and it is close to the Held et al.[8] rate at reference temperatures. When the formation rate of the lumped hexenyl radical decreases in favor of a higher 1-hexene concentration, the predicted peak concentration of 1,3-butadiene decreases by 5% of the MPC. Since the lumped hexenyl radical is formed mainly via the hydrogen abstraction from 1-hexene, changes in reactions involving 1-hexene also affect the prediction of 1,3-butadiene. For example, the predicted peak concentration of 1,3-butadiene increases by 13% of the MPC due to a higher concentration profile of 1-hexene after a slower 1-hexene thermal decomposition reaction (using the generic rate of reaction 1 in Table 1) is selected. 1-Butylene has an important effect on the concentration of 1,3-butadiene, since it is the major source of 3-butenyl (allylic) or 4-butenyl radicals, the decomposition reactions of which are the most important formation routes of 1,3-butadiene. A higher 1-butylene concentration after the modification of its thermal decomposition rate (reactions 2 and 3 in Table 1) increases the predicted peak concentration of 1,3-butadiene by 42% of the MPC.

Besides 1-hexene and 1-butylene, changes involving the allyl radical also affect the profile of 1,3-butadiene. The lower level of allyl radical due to various modifications, for example, reactions 1–3 in Table 1, reduces the predicted peak concentration of 1,3-butadiene by a total of 11% of the MPC in the *n*-heptane flame. With those modifications, the peak concentration of 1,3-butadiene in the *n*-heptane flame is overpredicted by 15%, as seen in Figure 4.

Allene. The predicted peak concentrations of allene in the *n*-decane and *n*-heptane flames using the Utah heptane mechanism are higher than the measured values by 12 and 231%, respectively. No modifications specifically targeted at allene were intended in the extended mechanism, but the concentration profiles of allene are affected significantly by changes in reactions involving other species, especially those involving the allyl radical. When the formation of various olefins is favored after the additions of olefin formation from β scission, or from larger olefin species via hydrogen addition followed by decomposition, the resulting higher levels of the allyl radical lead to the higher predicted peak concentrations of allene. These higher concentrations are results of hydrogen abstraction or thermal decomposition of the allyl radical and exceed the values measured in the *n*-decane and *n*-heptane flames by 42 and 33% of the MPC, respectively.[28] Although the gains in allene level lead to larger numerical deviations from the measured concentration profiles, they are offset by changes in reactions also involving the allyl radical after the formation rates of the allyl radical from thermal decomposition or hydrogen abstraction of olefins (reactions 1–3 in Table 1) are reduced. The decreased levels of the allyl radical lead to declines of allene concentrations in the *n*-decane and *n*-heptane flames of 66 and 143% of the MPC, respectively. Those changes in reactions involving the allyl radical yield better-predicted allene concentration profiles, especially in the *n*-heptane flame where the peak concentration of allene is now overpredicted by 100% compared to 230% before modifications.

Besides the allyl radical, changes in reactions involving other C_3H_5 isomers also affect the concentrations of allene. The predicted peak concentrations of allene in the *n*-decane and *n*-heptane flames are 16 and 39% of the MPC lower, respectively, after the enhanced formation of propyne from 2-propenyl radical ($CH_3{-}C{\bullet}{=}CH_2$) was selected (leaving out the third body species, as mentioned above). The modified reaction competes with that of allene from the same C_3H_5 isomer. The allene concentrations are slightly reduced when a new combination reaction of 2-propenyl and methyl radicals (reaction 5 in Table 1) is added to enhance the formation of isobutylene. Although the predicted maximum concentration of allene in the *n*-heptane flame has been greatly improved by modifying or adding reactions involving C_3H_5 isomers, it is still higher than the measured value by 97%. The prediction of allene in the *n*-decane flame is much better, with the peak concentration 18% lower than that of the experimental data. The effects of major modifications are shown in Figure 4.

Discussion

Few species have participated in reactions that have a greater impact on the concentrations of other species than the allyl radical $CH_2CH{=}CH_2$. For example, concentrations of higher olefins are very sensitive to changes in the thermal decomposition rates of these olefins to form the allyl radical, as seen for 1-heptene, 2-heptene, 3-heptene, 1-hexene, and 1-butylene. The concentration of propylene is determined by the partial equilibrium between propylene and the allyl radical via the following reactions of $C_3H_6 + X = CH_2{=}CH{-}CH_2 + HX$ and $CH_2{=}CH{-}CH_2 + H = C_3H_6$. The changes in the concentration of the allyl radical also affect that of allene, since the hydrogen abstraction from the allyl radical is the most important formation route for allene. The importance of the influence of the allyl radical on the propyne concentration cannot be overstated, since the majority of propyne is formed from the decomposition of the other two C_3H_5 isomers, and these isomers come mainly

from the allyl radical via isomerization for most fuels or from the decomposition of 2-butylene or isobutylene for some fuels as discussed earlier. Similar conclusions can be made for the concentrations of 2-butylene and isobutylene, since the combination of the methyl radical and propenyl isomers, other than the allyl radical, is their major formation route if the fuel does not include 2-butylene or isobutylene substructures.

Furthermore, changes in the concentration of the allyl radical have significant effects on those of C_4 unsaturated species via the intermediates of 1-butylene and the propargyl radical. For example, the concentrations of most C_4 species are affected by the change in the combination reaction of allyl and methyl radicals to form 1-butylene. In the *n*-decane flame, the predicted peak concentrations of 1,3-butadiene increase by 26% of the MPC because of a higher 1-butylene concentration, and a similar trend is also seen for the concentrations of this species in the *n*-heptane flame. Also seen is the influence of the allyl radical level on the concentration of 1-butyne via the intermediates of 1-butylene or the propargyl radical, since the combination of the propargyl and methyl radicals is the dominant formation route of 1-butyne, and the majority of the propargyl radicals are formed from the hydrogen abstraction from allene and propyne, and these C_3H_4 isomers are formed mainly from the allyl radical.

Acknowledgment. This research was funded by the University of Utah Center for the Simulation of Accidental Fires and Explosions (C-SAFE), through a contract with the Department of Energy, Lawrence Livermore National Laboratory (B341493).

EF700526N